Proceedings of the 17th World Congress
The International Federation of Automatic Control
Seoul, Korea, July 6-11, 2008

Fault Detection based on Orthotopic Set Membership Identification for Robot Manipulators

Vasso Reppa * **Anthony Tzes** *

* *Department of Electrical and Computer Engineering, University of Patras, Rio, Achaia, 26500, Greece (Tel: +30-2610-997293; e-mail: (reppa,tzes@ece.upatras.gr).*

Abstract: In this article a fault detection algorithm for capturing structural and/or sensor failures in robot manipulators is presented. The robot dynamics is linearizable with respect to a certain parameter. Using this linearizable representation, common faults in robot arms, such as failures of actuators or faulty sensor measurements, can be identified as variations encountered in the parameter vector. The proposed algorithm uses an Orthotopic Set Membership Identifier that defines the feasible parameter set and the parameters' bounds, within which the Weighted Recursive Least Square parameter estimate resides. An Uncertainty Output Predictor that generates the future region of faultless system operation. A fault is detected, when one of the following criteria below is validated: a) the WRLS parameter estimate resides out of the parameters's bounds, b) there is a sudden increase in the volume of the feasible set and c) the system's output is not within the predicted interval. Simulation studies are offered to test this fault detection methodology, customized to a two-link robot arm.

1. INTRODUCTION

From a general point of view, the fault diagnosis problem is concerned with the detection of time instants where there is a significant difference in the nominal system's behavior. The next step is the detection of the reason of the fault occurrence. In case of robot manipulators, De Luca et al. [2005] determine a fault as the unexpected behavior observed in its torques, when a technical failure occurs. Dixon et al. [2000], Shin et al. [1999] report a Fault Detection Scheme targeting failures of actuators or active bias to a sensor measurement etc. Similarly, a false operation in its workspace, because of accidental collision with unknown obstacles or manipulating an unknown load has been reported in De Luca et al. [2005] and Spong [2001], respectively.

The classical statistical methodology for fault detection is based on a fault indicator, or residual, which is computed via a specific model and observation, and defines a fault symptom De Luca et al. [2003], Yen et al. [2000], Greenwood [2005], Zhang et al. [2004]. This method is applied mostly in case of sensor failures in robot manipulators. On the other hand, the deterministic methodology for fault detection concerns set-membership approach, which takes into account a priori knowledge of model uncertainties and measurement errors Adrot et al. [2002], Milanese et al. [2003], Fagarasan et al. [2004], Ploix et al. [2001]. The goal of the set-membership approach is the characterization of a set of all parameter vectors that are consistent with the data, model structure and bounded noise errors, called feasible parameter set. In most techniques, the system output must be linearizable with respect to parameter vector. The benefit of the second methodology is the utilization of the parameter's intervals that arise from polytopes Chischi et al. [1998], Ingimundarson et al. [2005], bounding the feasible parameter set.

⋆ This work was partially supported by University of Patras' K. Karatheodoris research initiative program

In this paper, a Fault Detection (FD) algorithm based on the interactive relation of an Orthotopic Set Membership Identifier (OSMI) and an Uncertainty Output Predictor is presented. The OSMI uses two geometric approaches: the ellipsoid Cheung et al. [1993], Fogel et al. [1982], Milanese et al. [1982], for the characterization of the feasible parameter set and the orthotope Le et al. [1997], Tzes et al. [1999], bounding the ellipsoid, for the computation of parameters' bounds. The center of both the ellipsoid and the orthotope is the Weighted Recursive Least Square (WRLS)parameter estimate, and its volume reflects the parameter uncertainties, being induced from the bounded noise error. The vertices of the orthotope represent the parameter interval Walter et al. [1990], Fagarasan et al. [2001]. The bounds of the parameter interval are the inputs to the Uncertainty Iput/Output Predictor that generates the limited region of proper system operation. Finally, the fault detection is accomplished, when: a) the WRLS estimate of the parameter vector does not reside within the computed bounds, or b) the volume of the ellipsoid is suddenly increased Reppa et al. [2007] and c) the systems output is not within the predicted limited region Reppa et al. [2006].

This paper is structured in the following manner. The non linear system dynamics of a robot arm and the inherent assumptions that must be satisfied for the proper application of the FD-methodology are presented in the next section. The mathematical preliminaries of the OSMI is detailed in section 3, followed by the simulation studies and the conclusive remarks.

2. PROBLEM STATEMENT

The dynamic equation of an m-link robot manipulator is given from the Euler-Lagrange theory as:

$$M(q)\ddot{q} + C(q,\dot{q}) + G(q) = \tau \quad (1)$$

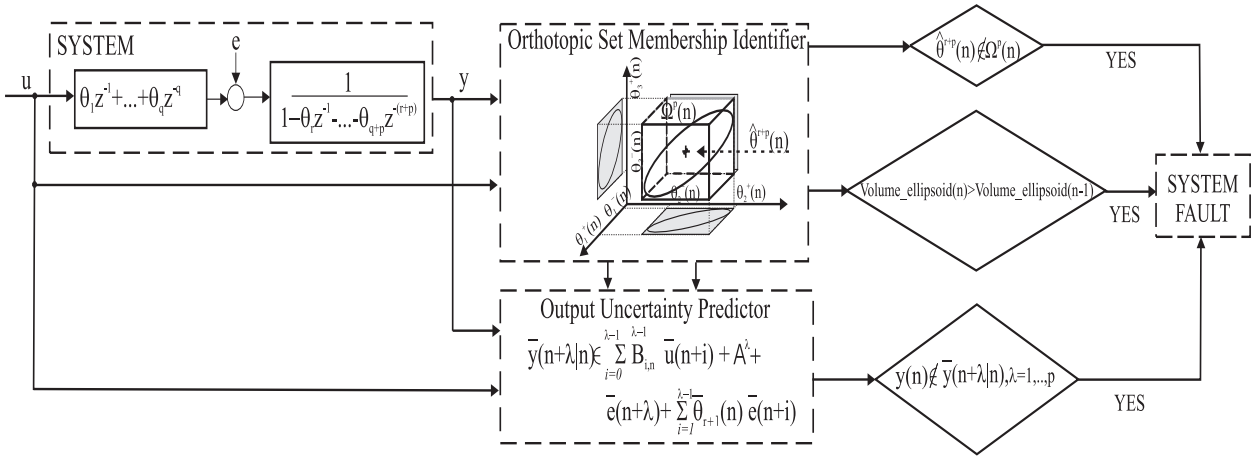

Fig. 1. Orthotopic Set Membership Identification Scheme

where $M(q) \in \Re^{m\times m}$ is the symmetric positive definite inertia matrix, $C(q,\dot{q}) \in \Re^{m\times m}$ is the Coriolis and centripetal matrix, $G(q) \in \Re^{m}$ is the gravitational vector and $\tau \in \Re^{m}$ are the applied torques.

Equation (1) can be formed as:

$$\tau = \theta^T Y(q,\dot{q},\ddot{q}) \tag{2}$$

where θ is a constant $(r+p)$-parameter vector and Y is an $(r+p)\times m$ matrix of known functions of the generalized coordinates and their derivatives $(q,\dot{q},\ddot{q})$. The above equation means that the Lagrangian dynamic equations are linear parametrizable.

It has to be underlined that the fault detection methodology is based on three rather "strict" assumptions:

1st assumption: The aforementioned nonlinear system is linearizable, with its discrete dynamics expressed in the most general form as

$$y(n) = \theta(n)^T \phi(n) + e(n),\ y(n), e(n) \in \Re^m \tag{3}$$

$$\phi(n) = \underbrace{\begin{bmatrix} \phi_1\left(u(n-1),\ldots,u(n-r),y(n-1),\ldots y(n-p)\right) \\ \phi_2\left(u(n-1),\ldots,u(n-r),y(n-1),\ldots y(n-p)\right) \\ \vdots \\ \phi_m\left(u(n-1),\ldots,u(n-r),y(n-1),\ldots y(n-p)\right) \end{bmatrix}^T}_{regression\ vector} \tag{4}$$

$$\theta(n) = \underbrace{[\theta_1(n),\ldots,\theta_r(n),\theta_{r+1}(n),\ldots,\theta_{r+p}(n)]^T}_{parameter\ vector} \tag{5}$$

2nd assumption: $\theta(n)$ remains constant over a sliding window with length L' or $\theta(n) = \theta(n-1) = ... = \theta(n-L')$. The window's minimum length, L^* is assumed to be known, whereas the time instants-(n_i) where the parameter vector can change (jump) $(\theta(n_i) \neq \theta(n_i-1))$ are unknown. This jump-parameter configuration is typical of systems prone to catastrophic faults.

3rd assumption: The noise sequence is point-to-point restricted, namely

$$\gamma_n \left\|e(n)\right\|^2 \leq 1, \forall n. \tag{6}$$

This noise sequence indirectly induces an uncertainty in the utilized identified model, $\hat{y}(n) = \hat{\theta}(n)\phi(n)$ and can be thought as the source of parametric uncertainty. Subsequently, interval bounds on the $\hat{\theta}(n)$ -parameter vector can be defined by mapping the noise-contaminated observations into uncertainty in the model.

The objective of the suggested FD-scheme, shown in Fig. 1, is to model "generic" faults of robot manipulator, such as system reconfiguration or accidental collision with unknown obstacles, as variations in parameter vector and to identify the time instants where these variations occur.

3. FAULT DETECTION BASED ON ORTHOTOPIC SET MEMBERSHIP IDENTIFICATION

3.1 Orthotopic Set Membership Identifier

Ellipsoid Definition: The intricacies behind the OSMI and its utilization in a fault detection scheme are presented in this section. The identified orthotope bounds an ellipsoid which contains the true parameter vector. The ellipsoid is

$$\begin{aligned} &\Omega(n) = \left\{\theta : (\theta - \hat{\theta}(n))^T \frac{C(n)}{\xi(n)} (\theta - \hat{\theta}(n)) \leq 1, \theta \in \Re^{r+p}\right\} \\ &C(n) = [\phi^{\mathrm{T}}(n)\phi(n)] \\ &\xi(n) = \hat{\theta}^T(n) C(n) \hat{\theta}(n) + \sum_{i=1}^{n} \frac{\lambda(i)}{\gamma_i}(1 - \gamma_i y^2(i)) \end{aligned} \tag{7}$$

where $\hat{\theta}(n)$ is the WRLS estimate of the parameter vector, $C(n)$ is the covariance matrix, and the symmetric positive definite matrix $W(n) = C(n)/\xi(n)$ determines how far the ellipsoid extends in each direction from $\hat{\theta}(n)$, and λ leads to the minimization of the ratio of the ellipsoid's volume at n and $n-1$, namely

$$\begin{aligned} &\lambda(n) \in \left\{\Re_0^+ : \min_{\lambda} \frac{\det(B(n))}{\det(B(n-1))}\right\}, \\ &B(n) = \overset{-1}{\det}\left(W(n)\right) \rightarrow \text{ellipsoid's "volume ratio"} \end{aligned} \tag{8}$$

Orhtotope Definition: In the sequel, the orthotope oriented parallel to the parameter coordinate axes and centered on the centroid of the ellipsoid, is computed via the equation [28]

$$\Omega^p(n) = \left\{\theta : \frac{1}{|\sigma_i(n)|}(\theta_i - \hat{\theta}_i(n)) \leq 1, i = 1,...,r+p\right\}. \tag{9}$$

The contact-points between the orthotope and the ellipsoid are

$$\begin{aligned} &\theta_i^- = \hat{\theta}_i - \sigma_i, \theta_i^+ = \hat{\theta}_i + \sigma_i \\ &\sigma_i = \sqrt{W_{i,i}^{-1}(n)}. \end{aligned} \tag{10}$$

and the orthotope's volume

$$V_{\text{orthotope}} = 2^{q+p}\sigma_1 \times \ldots \times \sigma_{r+p} \tag{11}$$

3.2 Uncertainty Output Predictor

The Uncertainty Output Predictor uses the vertices of the orthotope provided by the OSMI, as the inputs to the uncertainty-predictor for the computation of the λ-step ahead predicted output interval, which is given as:

$$\begin{aligned}\bar{y}(n+\lambda|n) &= \left[\hat{y}^-(n+\lambda|n), \hat{y}^+(n+\lambda|n)\right] \\ &= \bar{\theta}(n)\bar{\phi}(n+\lambda) + \bar{e}(n), \lambda \geq 1,\end{aligned} \tag{12}$$

where $\bar{e}(n) \in \left[-e^M(n), +e^M(n)\right]$ and $\gamma_n = 1\Big/\left(e^M\right)^2$ in (6). A recursive relationship is derived for generating the -step ahead predicted output interval, under the assumption that at time n, all past output quantities are known. The generic expression for $\bar{y}(n+\lambda|n), (1 \leq \lambda \leq p)$ is given as:

$$\begin{aligned}\bar{y}(n+\lambda|n) = &\sum_{i=0}^{\lambda-1} B_{i,n}^{\lambda-1}\bar{u}(n+i) + \mathrm{A}^{\lambda} + \bar{e}(n+\lambda) + \\ &\sum_{i=1}^{\lambda-1} \bar{\theta}_{q+i}(n)\bar{e}(n+i),\end{aligned} \tag{13}$$

where $A^{\lambda}, B_{i,n}^{\lambda}, i = 0, ..., \lambda-1$ are computed using the following recursive scheme:

$$\begin{aligned}
&B_{i,n}^{\lambda} = \sum_{j=1}^{\lambda-1} \theta_{q+j}(n) B_{i,n}^{\lambda-j} + \theta_{\lambda-1-i}(n), i = 0, \ldots \lambda-1 \\
&B_{0,n}^{1} = \theta_1(n), B_{1,n}^{1} = 0, i = 0, ..., \lambda-1 \\
&A^{\lambda} = \sum_{i=1}^{\lambda-1} \theta_{q+1}(n)A^i + \sum_{j=\lambda+1}^{q} \theta_j(n)u(n-j+\lambda) + \\
&\sum_{j=q+\lambda}^{q+p} \theta_j(n)y(n-j+q+\lambda-1), \lambda \geq 2 \\
&A^1 = \sum_{j=2}^{q} \theta_j(n)u(n-j+1) + \sum_{j=q+1}^{q+p} \theta_j(n)y(n-j+q)
\end{aligned} \tag{14}$$

3.3 Fault Detection Criteria

Using the Orthotopic Set Membership identifier and the Uncertainty Predictor Error, the FD-scheme recognizes a fault when:

(1) the centroid $\hat{\theta} \notin \Omega^p(n)$, or
(2) $\det(B(n)) > \det(B(n-1))$, or
(3) the actual $y(n)$ is not within the predicted intervals $y(n) \neq \bar{y}(n+i|n), i = 1, ..., \lambda$

4. SIMULATION STUDIES

The grasping of an unknown mass from a two-link robot arm, which is modelled as a sudden change in the mass of the second link is considered as a FD-instant. The two-link robot arm manipulating an unknown load is shown in Fig. 2, with m_1, m_2 being the masses of the links with I_1, I_2 the corresponding moments of inertia, and l_1, l_2, their lengths. The dynamic equations of the two-link robot are:

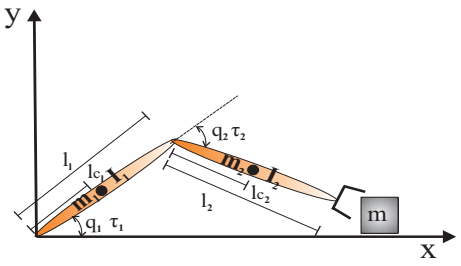

Fig. 2. Dual-link robot arm

$$\begin{bmatrix}\ddot{q}_1 \\ \ddot{q}_2\end{bmatrix} + h\begin{bmatrix}\dot{q}_1 \\ \dot{q}_2\end{bmatrix} + \begin{bmatrix}g_1 \\ g_2\end{bmatrix} = \begin{bmatrix}\tau_1 \\ \tau_2\end{bmatrix} \tag{15}$$

with

$$H = \begin{bmatrix}H_{11} & H_{12} \\ H_{21} & H_{22}\end{bmatrix}, h = \begin{bmatrix}-h\dot{q}_2 & -h\dot{q}_1 - h\dot{q}_2 \\ h\dot{q}_1 & 0\end{bmatrix} \tag{16}$$

$$\begin{aligned}
&H_{11} = m_1 lc_1^2 + I_1 + m_2\left(l_1^2 + lc_2^2 + 2l_1 lc_2 \cos q_2\right) + I_2 \\
&H_{22} = m_2 lc_2^2 + I_2 \\
&H_{12} = H_{21} = m_2 l_1 lc_2 \cos q_2 + m_2 lc_2^2 + I_2 \\
&h = m_2 l_1 lc_2 \sin q_2 \\
&g_1 = m_1 lc_1 g \cos q_1 + m_2 g\left(lc_2 \cos(q_1+q_2) + l_1 \cos q_1\right) \\
&g_2 = m_2 lc_2 g \cos(q_1+q_2)
\end{aligned} \tag{17}$$

where q_1, q_2 are the two joint angles and τ_1, τ_2 are the applied torques to the robot arm.

The suggested FD-scheme is applied to the system of the robot arm, whose parameters are presented in Table 1. The system under observation of the above two link robot

Table 1. Robot arm Kinematic and Dynamic parameters

m_1	m_2	l_1	l_2	lc_1	lc_2	I_1	I_2
10	5	1	1	0.5	0.5	0.833	0.416

is modeled as a MIMO ARMA system. It is assumed that the lengths of each link and the center of gravity of the first link are known and invariant. On the contrary, the masses of the two links and the center of gravity of the second link are unknown. The collection of system-relevant data over a time window $N \in [1, ..., n]$ that are inserted in the OSMI-scheme based on Eq. 2 and 3 generates:

$$\begin{bmatrix}\tau_1(1) \\ \tau_2(1) \\ \hline \vdots \\ \hline \tau_1(n) \\ \tau_2(n)\end{bmatrix}^T = \begin{bmatrix}\theta_1 \\ \theta_2 \\ \theta_3 \\ \theta_4\end{bmatrix}^T \begin{bmatrix}\Phi_1(1) \\ \Phi_2(1) \\ \hline \vdots \\ \hline \Phi_1(n) \\ \Phi_2(n)\end{bmatrix}^T + \begin{bmatrix}e_1(1) \\ e_2(1) \\ \hline \vdots \\ \hline e_1(n) \\ e_2(n)\end{bmatrix}^T, \tag{18}$$

where

$$\begin{aligned}\Phi_1 &= \left[\phi_{11}(1)\ \phi_{12}(1)\ \phi_{13}(1)\ \phi_{14}(1)\right], \\ \Phi_2 &= \left[\phi_{21}(1)\ \phi_{22}(1)\ \phi_{23}(1)\ \phi_{24}(1)\right]\end{aligned} \tag{19}$$

or,written in a compact form,

$$[\tau_i]_{1\times n} = \left[\theta^T\right]_{1x4}[\Phi_i]_{4\times n} + [e_i]_{1\times n} \tag{20}$$

The elements of the regression vector are

$$
\begin{aligned}
\phi_{11}(n) &= l_1^2\ddot{q}_1(n) + l_1 g\cos q_1(n),\\
\phi_{12}(n) &= l_1\left(\cos q_2\left(2\ddot{q}_1(n)+\ddot{q}_2(n)\right)\right)\\
&\quad - l_1\left(\sin q_2(n)\left(\dot{q}_2(n)^2 + 2\dot{q}_1(n)\dot{q}_2(n)\right)\right)\\
&\quad + l_1\left(g\cos(q_1(n)+q_2(n))\right),\\
\phi_{13}(n) &= \left(\frac{1}{12}l_1^2 + lc_1^2\right)\ddot{q}_1(n) + lc_1 g\cos q_1(n),\\
\phi_{14}(n) &= \ddot{q}_1(n) + \ddot{q}_2(n),\\
\phi_{21}(n) &= 0,\\
\phi_{22}(n) &= l_1\left(\cos q_2(n)\ddot{q}_1(n)\right) - l_1\left(\sin q_2(n)\dot{q}_1(n)^2\right)\\
&\quad + g\cos(q_1(n)+q_2(n)),\\
\phi_{23}(n) &= 0,\\
\phi_{24}(n) &= \ddot{q}_1(n) + \ddot{q}_2(n)
\end{aligned}
\tag{21}
$$

the elements of the parameter vector are

$$
\begin{aligned}
\theta_1 &= m_2,\\
\theta_2 &= m_2 lc_2,\\
\theta_3 &= m_1,\\
\theta_2 &= I_2 + m_2 lc_2^2
\end{aligned}
\tag{22}
$$

and finally the noise sequence $|e_i(n)| \leq e_i^M$.

4.1 Case study assumptions

The simulation studies are based on the above system representation for the first link ($[\tau_1]_{1\times n} = \left[\theta^T\right]_{1x4}[\Phi_1]_{4\times n} + [e_1]_{1\times n}$), which satisfies the first assumption for the application of the fault detection methodology. The reason of using only the system representation of the first link is that ϕ_{21}, ϕ_{23} are zeros and the corresponding θ_1, θ_3 cannot be identified and their bounds cannot be computed. The nominal values of the parameter vector are determined from the entries of Table 1. The set membership identification is realized taking into account that the noise error bound γ_n is constant and equals to $1\Big/\left(e_1^M\right)^2$. In this example, $e_1^M = 0.01|\tau_1|$ is the maximum noise bound for the first input and $|\tau_1| = 175.2$ is the magnitude of this input. In Fig. 3, the convergence of the four parameters to the aforementioned nominal values and the variation of the ellipsoid's volume are presented.

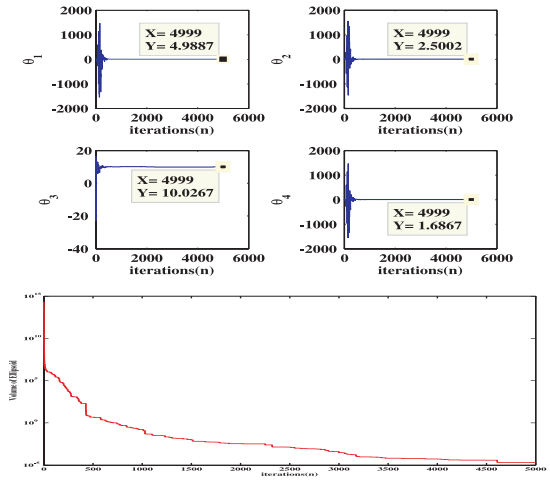

Fig. 3. WRLS estimate of the four parameters ($\theta_i, i = 1, ..., 4$) and the variation of ellipsoid's volume

For simulation purposes, it is assumed that the two-link robot arm suddenly grasps a load of mass, $m = 9 * m_2$ at the 2501^{st} time instant. The grasping of the unknown mass results in the increment of ${m_2}^{new} = 10 * m_2$. In addition, the applied torque does not equal to the model-based torque, expected in the absence of the collision. An issue of concern is the OSMI behavior after the mass increment.

4.2 Validation of the 1^{st} Fault Detection Criterion

The sudden variation in the mass of the second link of the robot arm is identified, after the "trigger" of the first fault detection criterion. Computing at every time instant the WRLS estimate of the parameter vector and its bounds, it is proven that before and after the 2501^{st} sample the estimate always resides within the parameter interval, except from this particular sample. The recognition of the fault occurrence and the time that this happens are shown in Figures 4-7. In each figure, the performance of the parameter $\hat{\theta}_i$, $i = 1, ..., 4$, the region of the fault occurrence and the logical fault indicator, which equals to one only if the parameter estimate is out of the computed bounds ($\hat{\theta}_i(n) > \theta_i^+(n)$ or $\hat{\theta}_i(n) < \theta_i^-(n)$) are presented.

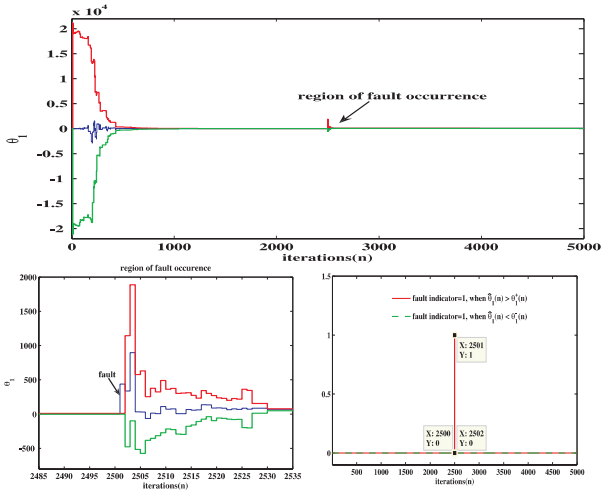

Fig. 4. Upper (red line) and lower (green line) bounds and the WRLS estimate (blue line) of the parameter θ_1 and the fault indicator

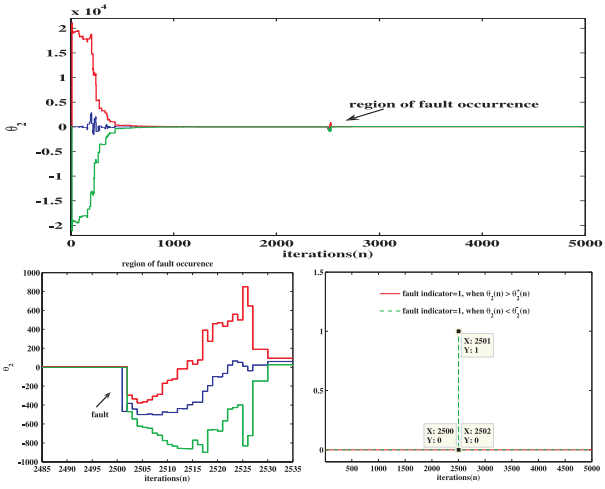

Fig. 5. Upper (red line) and lower (green line) bounds and the WRLS estimate (blue line) of the parameter θ_2 and the fault indicator

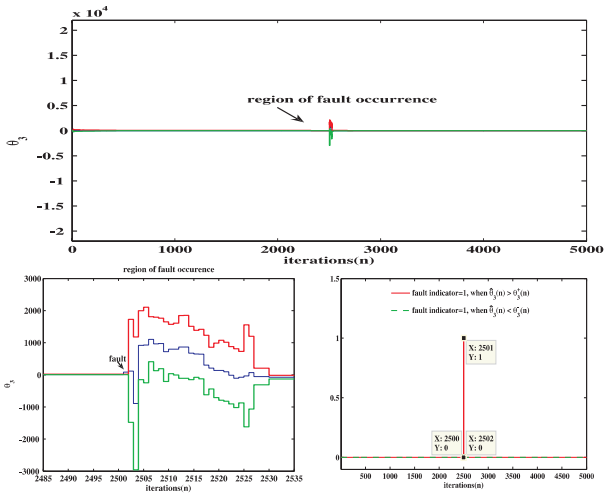

Fig. 6. Upper (red line) and lower (green line) bounds and the WRLS estimate (blue line) of the parameter θ_3 and the fault indicator

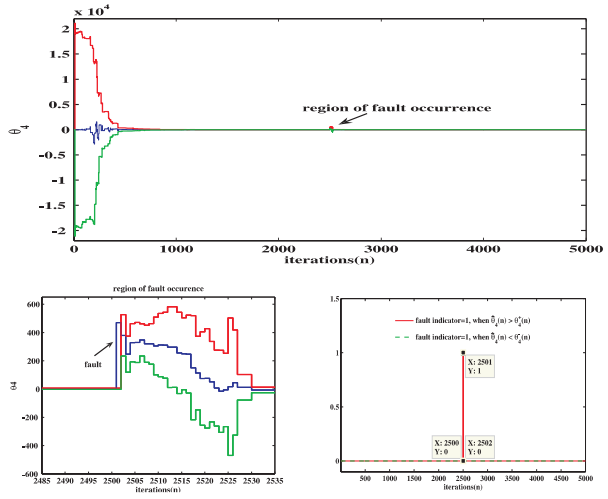

Fig. 7. Upper (red line) and lower (green line) bounds and the WRLS estimate (blue line) of the parameter θ_4 and the fault indicator

4.3 Validation of the 2^{nd} Fault Detection Criterion

The second criterion which leads to the detection of a faulty behavior of the system is the fact that the volume of the ellipsoid grows at the 2501^{st} time instant, as observed in Fig. 8. This fact objects to the basic presupposition of the deterministic algorithms that characterize the feasible parameter set via an ellipsoid, which is the reduction of the ellipsoid's volume at every time instant, as shown in Fig. 3. In Fig. 9, the ellipsoid and the orthotope, bounding the ellipsoid at the time instant $n = 2500$, are presented. On the other hand, at the time instant $n = 2501$, not only the orthotope does not bound the ellipsoid, but also the volume of the ellipsoid has been increased excessively in comparison with the volume of the orthotope, presented in Fig. 10.

4.4 Validation of the 3^{rd} Fault Detection Criterion

The detection of a "fault" in the behavior of the robot manipulator is also verified via the Uncertainty Output Predictor, defined in equation 13. It is already referred that the dynamic effect of the unexpected grasping is the augmentation of joint torques to the commanded ones.

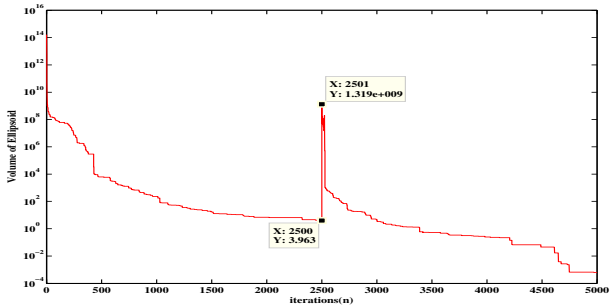

Fig. 8. Variation of ellipsoid's volume

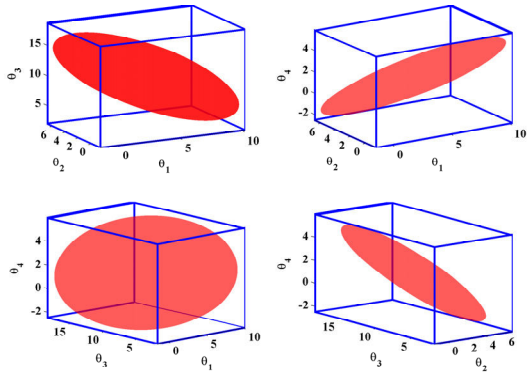

Fig. 9. Orthotope and ellipsoid representations prior to the fault

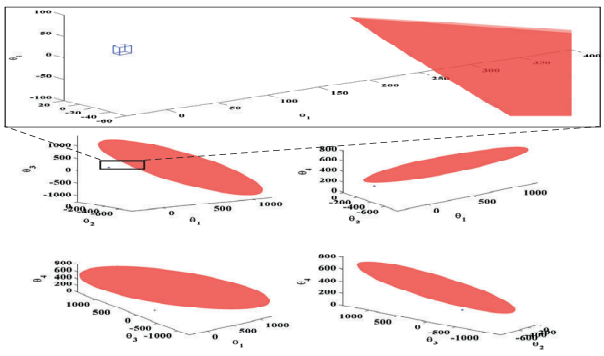

Fig. 10. Orthotope and ellipsoid representations after the fault

The variations in the joint torques can be predicted via the Uncertainty Output Predictor. The predicted upper and lower bound of the "new" torque of the first joint, and the actual one are presented in Fig. 11, for noise error bound $e_1^M = 0.01|\tau_1|$. In this Figure there is also a fault indicator, which is equal to 1, when $y(n) > y^+(n+\lambda|n)$ or $y(n) < y^-(n+\lambda|n)$.

5. CONCLUSION

A Fault Detection scheme is utilized for capturing sudden variations of the parameter vector encountered in the linearizable model of a robot arm. The primary goal is the parameter estimation of the system, when the data are corrupted by unknown but bounded error, consistent with the measurements, the model and the error description (feasible parameter set). A "false" performance is detected

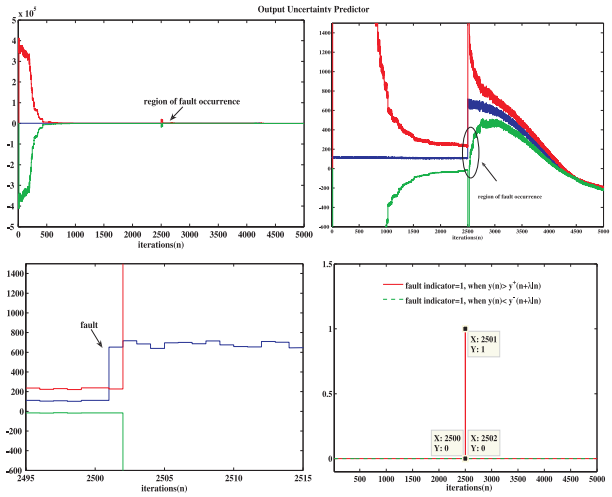

Fig. 11. The predicted upper(red line) and lower bound (green line) and the actual (input) torque of the first link (blue line) and the fault indicator

either when the WRLS estimate resides out of the bounds that are defined via the orthotopic set membership, or a sudden increase in the ellipsoid's volume of the feasible region, or when the predicted values of the robot's output vector are not within a certain interval. Simulation studies are used to investigate the efficiency of the presented algorithm.

REFERENCES

A. De Luca and R. Mattone, "An identification scheme for robot actuator faults". *In Proceedings of 2005 IEEE Internationan Conference of Intelligent Robots and Systems*, Edmonton, Alberta, Canada, pages 1127–1131, 2005.

W. Dixon, I. D. Walker, D. Dawson, and J. Hartranft, "Fault detection for robot manipulators with parametric uncertainty: A prediction-error-based approach". *IEEE Transactions on Robotics and Automation*, volume 16, number 6, December, 2000, pages 689–699.

J.-H. Shin and J.-J. Lee, "Fault detection and robust fault recovery control for robot manipulators with actuator failures". *In Proceedings of the 1999 IEEE International Conference on Robotics & Automation*, Kyongju, Korea, 1999, pages 861–865.

A. De Luca and R. Mattone, "Sensoreless robot collision detection and hybrid force/motion control". *In Proceedings of the 2005 IEEE International Conference on Robotics & Automation*, Barcelona, Spain, 2005, pages 999–1004.

M. W. Spong, "On the robust control of robot manipulators". *IEEE Transactions on Automatic Control*, volume 46, number 6, June, 2001 pages 853–865.

A. De Luca and R. Mattone, "Actuator failure detection and isolation using generalized momenta". *In Proceedings of the 2003 IEEE International Conference on Robotics & Automation*, Taipei, Taiwan, 2003, pages 634–639.

G. G. Yen and H. Liang-Wei, "Fault tolerant control: An intelligent sliding mode control strategy". *In Proceedings of the American Control Conference*, Chicago, Illinois, USA, 2000, pages 4204–4208.

G. Greenwood, "On the practicality of using reconfiguration for fault recovery". *IEEE Transactions in Evolutionary Eomputation*, volume 9, number 4, August, 2005, pages 398–405.

Z. Zhang, T. Parisini, and M. M. Polycarpou, "Adaptive fault-tolerant control of nonlinear uncertain systems: An information-based diagnostic approach". *IEEE Transactions in Automatic Control*, volume 49, number 8, August, 2004, pages 1259–1274.

O. Adrot, H. Janati-Idrissi and D. Maquin, "Fault detection based on interval analysis". *In Proceedings of the 15th IFAC World Congress*, Barcelona, Spain, 2002, pages 61–66.

M. Milanese, and C. Novara, "Learning complex systems from data: the set membership approach". *Multidisciplinary Research in Control: The Mohammed Dahleh Symposium 2002*, Springer Berlin / Heidelberg, 2003, pages 195–206.

I. Fagarasan, S. Ploix, and S. Gentil, "Causal fault detection and isolation based on set-membership approach". *Automatica*, volume 40, number 1, 2004, pages 2099–2110.

S. Ploix and C. Follot, "Fault diagnosis reasoning for set-membership approaches and application". *In Proceedings of the 2002 IEEE International Symposium on Intelligent Control*, Mexico City, Mexico, 2001, pages 85–90.

M.-F. Cheung, S. Yurkovich, and K. M. Passino, "An optimal volume ellipsoid algorithm for parameter set estimation". *IEEE Transactions in Automatic Control*, volume 38, number 8, August, 1993, pages 1292–1296.

E. Fogel and Y. F. Huang, "On the value of information in system identification-bounded noise case". *Automatica*, volume 18, number 2, March, 1982, pages 229–238.

M. Milanese and G. Belforte, "Estimation theory and uncertainty intervals evaluation in presence of unknown but bounded errors: linear families of models and estimators". *IEEE Transactions in Automatic Control*, volume 27, number2, April, 1982, pages 408–414.

K. Le, Z. Huang, C. W. Moon, and A. Tzes, "Adaptive thresholding-a robust fault detection control". *In Proceedings of the 36th IEEE Conference on Decision & Control*, San Diego, CA, USA, 1997,pages 4490–4495.

A. Tzes and K. Le, "Fault detection for jump discrete systems". *In Proceedings of the American Control Conference*, San Diego, CA, USA, 1999, pages 4496–4500.

E. Walter and H. Piet-Lahanier, "Estimation of parameter bounds from bounded-error data: a survey". *Mathematics and Computers in Simulation*, volume 32, number 5–6, December, 1990, pages 449–468.

I. Fagarasan, S. Ploix and S. Gentil, "Bounding approach for fault detection and diagnosis". *In Proceedings of IFAC Symposium large Scale Systems*, Bucarest, Romania, 2001.

V. Reppa and A. Tzes, "Fault Detection using Set Membership Identification for Micro-Electrostatic Actuators". *In Proceedings of the 2007 IEEE International Conference on Control Applications*, Singapore, 2007, pages 789–794.

V. Reppa and A. Tzes, "Application of Set Membership Identification for Fault Detection of MEMS". *In Proceedings of the 2006 IEEE International Conference on Robotics & Automation*, Orlando, Fl, USA, 2006, pages 643–648.

L. Chischi, A. Garulli, A. Vicino and G. Zappa, "Block recursive parallelotopic bounding in set membership identification". *Automatica*, volume 34, number 1, 1998, pages 15–22.

A. Ingimundarson, J. M. Bravo, V. Puig, and T. Alamo, "Robust fault diagnosis using parallelotope-based set-membership consistency tests". *In Proceedings of the 44th IEEE Conference on Decision & Control*, Seville, Spain, 2005, pages 993–998.

J. R Deller, "Set membership identification in digital signal processing". *The IEEE ASSP Magazine*, volume 6, number 4, October, pages 4–20.